2011 American Control Conference
on O'Farrell Street, San Francisco, CA, USA
June 29 - July 01, 2011

Nonlinear Dynamic Model and Stability Analysis of Self-Excited Induction Generators

Marc Bodson, *Fellow, IEEE,* and Oleh Kiselychnyk

Abstract— **The paper presents a nonlinear state-space model of a self-excited induction generator. A systematic methodology is then proposed to compute all the possible operating points and the eigenvalues of the linearized system around the operating points. In addition to a zero equilibrium, one or two operating points are typically found possible. In the first case, the zero equilibrium is unstable, resulting in spontaneous transition to the stable nonzero operating point. In the second case, the smaller of the nonzero operating points is unstable, so that only one stable operating point exists. However, the unstable operating point creates a barrier that must be overcome through triggering. The paper concludes with numerical examples and experiments illustrating the application of the theoretical results.**

Index Terms— **induction generator, self-excitation, nonlinear dynamic model, renewable energy, electric machines.**

I. Introduction

Induction generators have found applications in renewable energy (wind and hydro), due to their ability to generate electric power at frequencies that are not exactly tied to their frequency of rotation. The focus of the paper is on self-excited induction generators (SEIG), which generate power off-grid. There are two fundamental approaches to the analysis of self-excited generators. The first one is based on the steady-state equivalent circuit of the generator, where the total loop impedance [1]-[4] or the total node admittance at the magnetizing branch [5]-[7] is equated to zero. The condition is necessary to ensure the existence of a non-zero operating point. The second approach utilizes the generalized model of the induction machine [8]-[11] to search for parameters such that the system of differential equations describing the SEIG becomes unstable. The method assumes the existence of a stable, nonzero equilibrium where the trajectories converge. Analytic conditions replacing the extensive numerical computations of the eigenvalues of a 6X6 matrix associated with the linear model of the SEIG were derived in [12].

Research on SEIG [13]-[15] has shown the necessity to take into account the non-linearity of the magnetizing inductance not only in the high current region (magnetic saturation), but also in the low current region. The nonlinear magnetizing curve can be incorporated in a dynamic model in different ways, and authors have typically used an ad-hoc model obtained by replacing the magnetizing inductance of a linear model by the nonlinear function. In contrast, Levi [16][17] has proposed a model of saturation that is better justified theoretically, although more complicated.

This paper uses Levi's model to obtain a nonlinear state-space model of the induction generator taking into consideration the magnetic nonlinearity for both the high and the low current regions. An analysis of the possible operating points is derived, including an assessment of their stability properties and their regions of attraction. A new distinction is made between spontaneous and triggered self-excitation. Overall, the results connect the two fundamental approaches of self-excited induction generators.

Manuscript received September 26, 2010. This work was supported in part by the U.S. Department of State under Fulbright Grant 68431809.

M. Bodson is with the ECE Department, University of Utah, Salt Lake City, UT 84112, bodson@eng.utah.edu

O. Kiselychnyk is with the FEA Faculty, National Technical University of Ukraine "Kiev Polytechnic Institute", Kiev, Ukraine, 03056, koi@gala.net

II. Analytical Results

A. Mathematical Model of an Induction Generator

The standard model of a two-phase induction generator in an arbitrary coordinate frame consists of the vector differential equations

$$\frac{d\Psi_S}{dt} = U_S - R_S i_S - \omega_e J \Psi_S\,,\ J = \begin{bmatrix} 0 & -1 \\ 1 & 0 \end{bmatrix}$$

$$\frac{d\Psi_R}{dt} = -R_R i_R + (n_p\omega - \omega_e) J \Psi_R\,, \qquad (1)$$

where $\Psi_S = \begin{bmatrix}\Psi_{SF} & \Psi_{SG}\end{bmatrix}^T$, $\Psi_R = \begin{bmatrix}\Psi_{RF} & \Psi_{RG}\end{bmatrix}^T$ are vectors of stator and rotor total flux linkages, $i_S = \begin{bmatrix} i_{SF} & i_{SG}\end{bmatrix}^T$, $i_R = \begin{bmatrix} i_{RF} & i_{RG}\end{bmatrix}^T$ are vectors of stator and rotor currents, $U_S = \begin{bmatrix} U_{SF} & U_{SG}\end{bmatrix}^T$ is a vector of stator voltages, R_S and R_R are the stator and rotor resistances, n_p is the number of pole pairs, ω is the angular velocity of the rotor, and ω_e is the angular velocity of the arbitrary coordinate frame. Resistive loads are connected in parallel with capacitors to the stator windings, resulting in the additional vector equation

$$-C\frac{dU_S}{dt} = i_S + Y_L U_S + \omega_e C J U_S\,, \qquad (2)$$

where Y_L is the admittance of the resistive load and C is the value of the capacitor (both added to each phase).

The F and G indices denote the components associated with the rotating coordinate frame. For the stator currents,

$$\begin{pmatrix} i_{SF} \\ i_{SG} \end{pmatrix} = \begin{pmatrix} \cos(\theta_e) & \sin(\theta_e) \\ -\sin(\theta_e) & \cos(\theta_e) \end{pmatrix} \begin{pmatrix} i_{SA} \\ i_{SB} \end{pmatrix}, \qquad (3)$$

where i_{SA}, i_{SB} are the currents in the windings A and B and θ_e is the angle of the coordinate frame with respect to the A

winding. A similar expression applies for the voltages. For the rotor currents, θ_e is replaced by $\theta_e - n_P\,\theta$, where θ is the angular position of the rotor. The angular velocities are given by $\omega_e = d\theta_e/dt$ and $\omega = d\theta/dt$. In the case of a three-phase generator, a three-phase to two-phase transformation can be used to apply the results.

The magnetizing current of the induction generator is the sum of the stator current and the rotor current. The amplitude of the magnetizing current is

$$i_M = \sqrt{i_{MF}{}^2 + i_{MG}{}^2}\,,\; i_{MF} = i_{SF} + i_{RF}\,,\; i_{MG} = i_{SG} + i_{RG}\,. \tag{4}$$

Following the approach of [16], [17], the stator and rotor flux linkages are assumed to be of the form

$$\Psi_S = L_{\sigma S} i_S + L_M (i_S + i_R)\,,\; \Psi_R = L_{\sigma R} i_R + L_M (i_S + i_R)\,, \tag{5}$$

where $L_{\sigma S}$ and $L_{\sigma R}$ are the stator and rotor leakage inductances, and L_M is the stator-rotor mutual inductance, also called *magnetizing inductance*. Generally, saturation of the leakage inductances is neglected and the magnetizing inductance is solely considered a nonlinear function of the magnetizing current with

$$L_M = \Psi_M / i_M\,, \tag{6}$$

where Ψ_M denotes the amplitude of the main magnetic flux linkage. We have

$$\frac{dL_M}{di_M} = \frac{d\left(\Psi_M / i_M\right)}{di_M} = \frac{L - L_M}{i_M}\,, \tag{7}$$

where we defined

$$L = d\Psi_M / di_M = L_M + i_M\, dL_M / di_M\,, \tag{8}$$

as the *dynamic magnetizing inductance*. The magnetizing inductance and the dynamic magnetizing inductance are equal for a linear magnetic circuit, but not otherwise.

The time-derivative of the magnetizing current amplitude is

$$\frac{di_M}{dt} = \frac{1}{2i_M}\frac{d(i_{MF}^2 + i_{MG}^2)}{dt} = \frac{i_{MF}}{i_M}\frac{di_{MF}}{dt} + \frac{i_{MG}}{i_M}\frac{di_{MG}}{dt}\,, \tag{9}$$

so that the time-derivative of the magnetizing inductance becomes

$$\frac{dL_M}{dt} = \frac{dL_M}{di_M}\frac{di_M}{dt} = \frac{(L - L_M)}{i_M^2}\left(i_{MF}\frac{di_{MF}}{dt} + i_{MG}\frac{di_{MG}}{dt}\right). \tag{10}$$

Using these expressions in the time-derivatives of the stator and rotor flux linkages

$$\begin{aligned}
\frac{d\Psi_S}{dt} &= (L_{\sigma S} + L_M)\frac{di_S}{dt} + L_M\frac{di_R}{dt} + \frac{dL_M}{dt}(i_S + i_R)\,,\\
\frac{d\Psi_R}{dt} &= (L_{\sigma R} + L_M)\frac{di_R}{dt} + L_M\frac{di_S}{dt} + \frac{dL_M}{dt}(i_S + i_R)\,,
\end{aligned} \tag{11}$$

one obtains the model of the induction generator in the form of the implicit nonlinear differential matrix equation

$$E\dot{X} = FX\,, \tag{12}$$

where

$$E = \begin{bmatrix}
-C & 0 & 0 & 0 & 0 & 0\\
0 & L_{\sigma S} + L_{MF} & L_{MF} & 0 & L_{MFG} & L_{MFG}\\
0 & L_{MF} & L_{\sigma R} + L_{MF} & 0 & L_{MFG} & L_{MFG}\\
0 & 0 & 0 & -C & 0 & 0\\
0 & L_{MFG} & L_{MFG} & 0 & L_{\sigma S} + L_{MG} & L_{MG}\\
0 & L_{MFG} & L_{MFG} & 0 & L_{MG} & L_{\sigma R} + L_{MG}
\end{bmatrix},$$

$$F = \begin{bmatrix}
Y_L & 1 & 0 & -C\omega_e & 0 & 0\\
1 & -R_S & 0 & 0 & \omega_e(L_{\sigma S} + L_M) & \omega_e L_M\\
0 & 0 & -R_R & 0 & \left(\omega_e - n_p\omega\right)L_M & \left(\omega_e - n_p\omega\right)(L_{\sigma R} + L_M)\\
C\omega_e & 0 & 0 & Y_L & 1 & 0\\
0 & -\omega_e(L_{\sigma S} + L_M) & -\omega_e L_M & 1 & -R_S & 0\\
0 & \left(n_p\omega - \omega_e\right)L_M & \left(n_p\omega - \omega_e\right)(L_{\sigma R} + L_M) & 0 & 0 & -R_R
\end{bmatrix},$$

$$X = \left[U_{SF}\; i_{SF}\; i_{RF}\; U_{SG}\; i_{SG}\; i_{RG}\right]^T, \tag{13}$$

and

$$\begin{aligned}
&L_{MF} = L_M + (L - L_M) i_{MF}^2 / i_M^2\,,\; L_{MG} = L_M + (L - L_M) i_{MG}^2 / i_M^2\\
&L_{MFG} = (L - L_M) i_{MF} i_{MG} / i_M^2\,.
\end{aligned} \tag{14}$$

Note that E and F are nonlinear functions of X through L_M, L_{MF}, L_{MG}, and L_{MFG}. Equation (12) can be transformed into the standard explicit form

$$\dot{X} = AX\,, \tag{15}$$

by defining $A = E^{-1}F$. In this form, standard numerical integration methods can be used. However, the system remains a nonlinear system, since A is a function of X.

An interesting alternative representation of the model can be obtained by using the following equalities

$$\begin{aligned}
&(L_{MF} - L_M)\left(\frac{di_{SF}}{dt} + \frac{di_{RF}}{dt}\right) + L_{MFG}\left(\frac{di_{SG}}{dt} + \frac{di_{RG}}{dt}\right)\\
&\quad = (L - L_M)\frac{i_{MF}}{i_M}\frac{di_M}{dt}\,,
\end{aligned} \tag{16}$$

$$\begin{aligned}
&(L_{MG} - L_M)\left(\frac{di_{SG}}{dt} + \frac{di_{RG}}{dt}\right) + L_{MFG}\left(\frac{di_{SF}}{dt} + \frac{di_{RF}}{dt}\right)\\
&\quad = (L - L_M)\frac{i_{MG}}{i_M}\frac{di_M}{dt}\,.
\end{aligned} \tag{17}$$

Substituting (16) and (17) into (12) and (13) gives the matrix equation

$$E_L\dot{X} = FX - \frac{L - L_M}{i_M}\frac{di_M}{dt}X_M\,, \tag{18}$$

where $X_M = \left[0\; i_{MF}\; 0\; i_{MG}\right]^T$ and

$$E_L = \begin{bmatrix}
-C & 0 & 0 & 0 & 0 & 0\\
0 & L_{\sigma S} + L_M & L_M & 0 & 0 & 0\\
0 & L_M & L_{\sigma R} + L_M & 0 & 0 & 0\\
0 & 0 & 0 & -C & 0 & 0\\
0 & 0 & 0 & 0 & L_{\sigma S} + L_M & L_M\\
0 & 0 & 0 & 0 & L_M & L_{\sigma R} + L_M
\end{bmatrix}. \tag{19}$$

Note that

$$E_L\dot{X} = FX\,. \tag{20}$$

is the model of the induction generator with linear magnetics, which is indeed verified since $L = L_M$ in that case. However, the second term of (18) also drops out if $di_M/dt = 0$. In other words, if a solution of (20) is obtained for which the

magnetizing current is constant, it is also a solution of the nonlinear system (18). This justifies the use of the linear model (19)-(20) with L_M a function of i_M to obtain steady-state responses but one should remember that the general dynamic model is more complicated.

B. Determination of possible operating modes

The determination of an operating mode can be performed by finding a periodic steady-state solution to the induction generator model in the stator frame of reference (ω_e=0). Alternatively, one can use the (equivalent) approach that consists in finding a frequency ω_e^* such that a *constant* solution exists in a rotating frame of reference. With either (12) or (18), the condition for such a constant solution is that there exists a vector X^* such that

$$F^* X^* = 0, \tag{21}$$

where F^* is the function F evaluated at the equilibrium X^* and at the frequency ω_e^* to be determined. The matrix F^* has the special structure

$$F^* = \begin{bmatrix} F_1^* & -F_2^* \\ F_2^* & F_1^* \end{bmatrix}, \tag{22}$$

so that for X^* partitioned similarly $X^* = \begin{bmatrix} X_1^* & X_2^* \end{bmatrix}^T$, equation (21) becomes

$$F_1^* X_1^* - F_2^* X_2^* = 0,\ F_2^* X_1^* + F_1^* X_2^* = 0. \tag{23}$$

The existence of a nonzero vector X^* such that (21) is satisfied is thus equivalent to the existence of a nonzero complex vector $Z^* = X_1^* + jX_2^*$ such that

$$\left(F_1^* + jF_2^*\right) Z^* = 0, \tag{24}$$

which occurs if and only if $\det(F_1^* + jF_2^*) = 0$. Using (13),

$$F_1^* + jF_2^* = \begin{bmatrix} Y_L + jC\omega_e^* & 1 & 0 \\ 1 & -R_S - j\omega_e^*(L_{\sigma S} + L_M^*) & -j\omega_e^* L_M^* \\ 0 & j\left(n_p\omega - \omega_e^*\right)L_M^* & -R_R + j\left(n_p\omega - \omega_e^*\right)(L_{\sigma R} + L_M^*) \end{bmatrix}, \tag{25}$$

so that the real and imaginary parts of $\det(F_1^* + jF_2^*) = 0$ are equal to

$$\begin{aligned} \mathrm{Re}\left(\det\left(F_1^* + jF_2^*\right)\right) &= c_1 L_M^* + c_2 = 0, \\ \mathrm{Im}\left(\det\left(F_1^* + jF_2^*\right)\right) &= c_3 L_M^* + c_4 = 0, \end{aligned} \tag{26}$$

where c_1, c_2, c_3 and c_4 are given by

$$\begin{aligned} c_1 &= -\omega_e^{*2} C R_R - \omega_e^*\left(\omega_e^* - n_p\omega\right)\left(Y_L L_{\sigma S} + Y_L L_{\sigma R} + C R_S\right), \\ c_2 &= R_R\left(1 + Y_L R_S\right) - \omega_e^{*2} C R_R L_{\sigma S} \\ &\quad - \omega_e^*\left(\omega_e^* - n_p\omega\right) L_{\sigma R}\left(Y_L L_{\sigma S} + C R_S\right), \\ c_3 &= \omega_e^* Y_L R_R - \left(\omega_e^* - n_p\omega\right)\left(\omega_e^{*2} C\left(L_{\sigma S} + L_{\sigma R}\right) - Y_L R_S - 1\right), \\ c_4 &= \omega_e^* C R_S R_R + \omega_e^* Y_L R_R L_{\sigma S} \\ &\quad - \left(\omega_e^* - n_p\omega\right)\left(\omega_e^{*2} C L_{\sigma S} L_{\sigma R} - Y_L R_S L_{\sigma R} - L_{\sigma R}\right). \end{aligned} \tag{27}$$

The two unknowns that must be determined using the two conditions in (26) are the frequency ω_e^* and the magnetizing inductance L_M^* (which in turn gives the magnetizing current i_M^* corresponding to the steady-state). One way to solve the equations is to eliminate L_M^* from (26), which results in a 5th order polynomial equation in ω_e^*

$$\begin{aligned} &C^2\left(R_S L_{\sigma R}^2 + R_R L_{\sigma S}^2\right)\omega_e^{*5} - n_p\omega C^2\left(2R_S L_{\sigma R}^2 + R_R L_{\sigma S}^2\right)\omega_e^{*4} \\ &+\left(\left(n_p\omega\right)^2 C^2 R_S L_{\sigma R}^2 + C^2 R_R^2 R_S + C^2 R_R R_S^2 - 2C R_R L_{\sigma S}\right. \\ &\left.+Y_L^2 R_S L_{\sigma R}^2 + Y_L L_{\sigma R}^2 + Y_L^2 R_R L_{\sigma S}^2\right)\omega_e^{*3} - n_p\omega\left(C^2 R_R R_S^2\right. \\ &\left.-2C R_R L_{\sigma S} + 2Y_L^2 R_S L_{\sigma R}^2 + 2Y_L L_{\sigma R}^2 + Y_L^2 R_R L_{\sigma S}^2\right)\omega_e^{*2} \\ &+\left(Y_L R_S + 1\right)\left(R_R + Y_L R_R^2 + \left(n_p\omega\right)^2 L_{\sigma R}^2 Y_L + Y_L R_S R_R\right)\omega_e^* \\ &-n_p\omega R_R\left(Y_L R_S + 1\right)^2 = 0. \end{aligned} \tag{28}$$

Although up to five solutions are possible, computations with realistic motor parameters typically yield at most one real positive solution ω_e^*. Substitution of ω_e^* in either equation of (26) then gives L_M^*. One or more values of i_M^* may be possible for a given L_M^*, depending on the shape of the magnetizing curve.

It remains to characterize the solutions in terms of X^*, so that stability of the equilibrium points can be assessed. With $U_S^* = U_{SF}^* + jU_{SG}^*$, $i_S^* = i_{SF}^* + ji_{SG}^*$, $i_R^* = i_{RF}^* + ji_{RG}^*$, and $Z^* = \left[U_S^*, i_S^*, i_R^*\right]^T$, the first two rows of (24) give (using (25))

$$\begin{aligned} i_S^* &= -\left(Y_L + jC\omega_e^*\right)U_S^*, \\ i_R^* &= \frac{\left(1 + \left(Y_L + jC\omega_e^*\right)\left(R_S + j\omega_e^*(L_{\sigma S} + L_M^*)\right)\right)}{j\omega_e^* L_M^*} U_S^*. \end{aligned} \tag{29}$$

The third row of (24) is linearly dependent on the first two rows, due to $\det(F_1^* + jF_2^*) = 0$, and does not give any additional condition. On the other hand, the fact that $i_M^* = \left|i_S^* + i_R^*\right|$ implies (using (29)) that

$$\left|U_S^*\right| = \frac{\omega_e^* L_M^* i_M^*}{\sqrt{(1 + Y_L R_S - C\omega_e^{*2} L_{\sigma s})^2 + \omega_e^{*2}(Y_L L_{\sigma s} + C R_S)^2}}. \tag{30}$$

An equilibrium vector X^* is characterized by a voltage U_S^* of arbitrary angle and magnitude given by (30), and currents i_S^*, i_R^* given by (29). There are an infinite number of equilibrium points, which are all identical except for a shift in angle of the generated voltages and currents (the relative phases remain the same).

C. Stability of operating modes

It would be tempting to assume that the stability of the system linearized around an equilibrium point X^* is determined by the eigenvalues of the matrix $A^*=(E^*)^{-1}F^*$. However, this is not correct if $X^* \neq 0$. The stability of the nonlinear system in the vicinity of X^* can be determined by

considering small perturbations δX with $X = X^* + \delta X$. For such perturbations around the equilibrium, a first-order description is

$$\left(E^* + \left[\frac{\partial E}{\partial X}\right]^* \delta X\right)\left(\dot{X}^* + \delta\dot{X}\right)$$
$$= \left(F^* + \left[\frac{\partial F}{\partial X}\right]^* \delta X\right)\left(X^* + \delta X\right), \quad (31)$$

where E^* and F^* are the values of the matrices E and F at the equilibrium and

$$\left[\frac{\partial E}{\partial X}\right]^* \delta X = \sum_{k=1}^{n}\left[\frac{\partial E}{\partial X_k}\right]^* \delta X_k \ . \quad (32)$$

The term in the second bracket is the matrix obtained by taking the partial derivative of the matrix E with respect to the k^{th} element of X and evaluating the elements of the resulting matrix at the equilibrium values. The summation is performed over the n elements of δX. A similar definition applies for F.

Using the fact that $\dot{X}^* = 0$ and $F^* X^* = 0$, and neglecting second-order terms, one obtains the linearized description of the system around the equilibrium

$$E^*\delta\dot{X} = F^*\delta X + \left[\frac{\partial F}{\partial X}\right]^* \delta X\, X^* . \quad (33)$$

Equation (33) can be put in the form

$$E^*\delta\dot{X} = \left(F^* + \delta F^*\right)\delta X , \quad (34)$$

where the $(i,j)^{th}$ element of the matrix δF^* is given by

$$\delta F_{ij}^* = \sum_{k=1}^{n}\left[\frac{\partial F_{ik}}{\partial X_j}\right]^* X_k^* . \quad (35)$$

If E^* is non-singular, the equilibrium vector X^* is stable if and only if all the eigenvalues of the matrix

$$A^* = \left(E^*\right)^{-1}\left(F^* + \delta F^*\right) \quad (36)$$

are in the open left-half plane.

For the induction generator, E^* and F^* are obtained by replacing the inductances L_M, L_{MF}, L_{MG}, and L_{MFG} in (13) by the equilibrium values and by replacing ω_e by ω_e^*. δF^* is given by

$$\delta F^* = \begin{bmatrix} 0 & 0 & 0 \\ 0 & \omega_e^*\delta_5 & \omega_e^*\delta_6 \\ 0 & (\omega_e^* - n_p\omega)\delta_5 & (\omega_e^* - n_p\omega)\delta_6 \\ 0 & 0 & 0 \\ 0 & -\omega_e^*\delta_1 & -\omega_e^*\delta_2 \\ 0 & (n_p\omega - \omega_e^*)\delta_1 & (n_p\omega - \omega_e^*)\delta_2 \end{bmatrix}$$
$$\begin{bmatrix} 0 & 0 & 0 \\ 0 & \omega_e^*\delta_3 & \omega_e^*\delta_4 \\ 0 & (\omega_e^* - n_p\omega)\delta_3 & (\omega_e^* - n_p\omega)\delta_4 \\ 0 & 0 & 0 \\ 0 & -\omega_e^*\delta_7 & -\omega_e^*\delta_8 \\ 0 & (n_p\omega - \omega_e^*)\delta_7 & (n_p\omega - \omega_e^*)\delta_8 \end{bmatrix}, \quad (37)$$

where

$$\delta_1 = \left(\frac{\partial L_M}{\partial i_{SF}}\right)^* i_{MF}^* , \quad \delta_2 = \left(\frac{\partial L_M}{\partial i_{RF}}\right)^* i_{MF}^* , \quad \delta_3 = \left(\frac{\partial L_M}{\partial i_{SG}}\right)^* i_{MG}^* ,$$
$$\delta_4 = \left(\frac{\partial L_M}{\partial i_{RG}}\right)^* i_{MG}^* , \quad \delta_5 = \left(\frac{\partial L_M}{\partial i_{SF}}\right)^* i_{MG}^* , \quad \delta_6 = \left(\frac{\partial L_M}{\partial i_{RF}}\right)^* i_{MG}^* ,$$
$$\delta_7 = \left(\frac{\partial L_M}{\partial i_{SG}}\right)^* i_{MF}^* , \ \delta_8 = \left(\frac{\partial L_M}{\partial i_{RG}}\right)^* i_{MF}^* . \quad (38)$$

The terms in parentheses can be determined using

$$\left(\frac{\partial L_M}{\partial i_{SF}}\right)^* = \left(\frac{dL_M}{di_M}\right)^*\left(\frac{\partial i_M}{\partial i_{SF}}\right)^* = \left(\frac{\partial L_M}{\partial i_{RF}}\right)^* = \frac{L^* - L_M^*}{i_M^*}\frac{i_{MF}^*}{i_M^*} , \quad (39)$$

and similarly for i_{SG}, i_{RG}.

Note that an arbitrary equilibrium vector can be transformed through a shift of angle in the FG reference frame into an equilibrium vector with $i_{MF}^* = i_M^*$, $i_{MG}^* = 0$. In this case, E^* and F^* are obtained by setting $L_{MF}^* = L^*$, $L_{MG}^* = L_M^*$, $L_{MFG}^* = 0$ while, in (37),

$$\delta_1 = \delta_2 = L^* - L_M^* , \ \delta_3 = \delta_4 = \delta_5 = \delta_6 = \delta_7 = \delta_8 = 0 . \quad (40)$$

Because all equilibrium vectors X^* associated with some ω_e^* and i_M^* can be transformed into the same equilibrium vector by a rotation of the reference axes, the systems linearized around all equilibrium vectors must have the same eigenvalues. For this reason, we will talk about "the" equilibrium point associated with a given ω_e^* and i_M^*, even though there are technically infinitely many (all equivalent) such equilibrium states.

D. General characteristics of operating modes

Fig. 1 shows the general shape of a magnetizing inductance as a function of the magnetizing current. The curve includes an ascending part rising from L_{MO} to L_{MAX}, a (more or less) flat part at L_{MAX} corresponding to a linear magnetic regime, and a descending part corresponding to magnetic saturation. Often, the ascending part of the curve is neglected (L_{MO}=L_{MAX}). However, several works [13]-[15] have shown the need to represent this nonlinearity at low currents to accurately model self-excitation in induction generators.

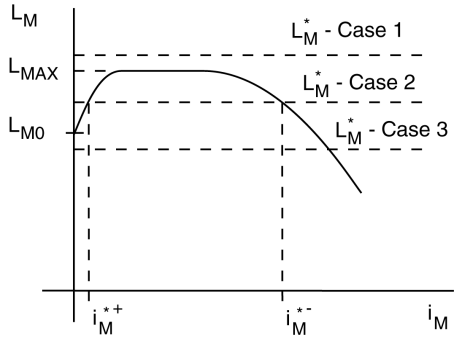

Fig. 1. Magnetization curve and three possible cases of steady-state values.

Three cases are shown on the figure:

- Case 1: with $L_M^* > L_{MAX}$, the generator has only one equilibrium state corresponding to $i_M^* = 0$.
- Case 2: with $L_{MAX} > L_M^* > L_{M0}$, the generator has three equilibrium states: $i_M^* = 0$, i_M^{*+} corresponding to the ascending part of the curve, and i_M^{*-} corresponding to the descending part of the curve.
- Case 3: with $L_{M0} > L_M^*$, the generator has two equilibrium states $i_M^* = 0$ and i_M^{*-} corresponding to the descending part of the curve.

Computations and experimental results to be presented hereafter have shown the following properties:

- Case 1: the equilibrium corresponding to $i_M^* = 0$ is stable.
- Case 2: the equilibrium corresponding to $i_M^* = 0$ and i_M^{*-} are stable. The equilibrium corresponding to i_M^{*+} is unstable.
- Case 3: the equilibrium state corresponding to $i_M^* = 0$ is unstable and the equilibrium corresponding to i_M^{*-} is stable.

In case 1, a power generating mode of self-excitation is not possible. In case 3, a power generating mode of self-excitation is possible and will naturally develop, due to the instability of the zero state. We refer to this condition as *spontaneous self-excitation*. In case 2, two power generating modes exist. The one associated with the lower magnetizing current is unstable, and cannot be sustained indefinitely (although experiments show that it may for some extended periods of time). If the unstable state is reached, small perturbations will either make the magnetizing current grow, resulting in the equilibrium state with higher magnetizing current to be reached, or to decay, resulting in a collapse of the voltage. Since, the zero state is stable: the generator will not naturally leave this state.

Simulations and experiments have shown that, to reach the stable power generating mode, the magnetizing current must be brought to a value greater than or equal to i_M^{*+}. This condition can be achieved, for example, by applying sufficiently large initial voltages to the capacitors. We refer to this condition as *triggered self-excitation*. Sometimes, it is also possible for residual magnetization to produce the result.

III. Experimental Results

A. Operating modes

Experimental results were obtained for a small two-phase induction motor (Bodine KCI-22A1, with rated values 7.5W, 24V, 60 Hz, and 3350 rpm). The parameters and analytical approximations of $L_M=f(i_M)$ and $L=f(i_M)$ were determined in [15]. The induction motor was tested as a generator by coupling it to a DC motor/tachometer under closed-loop velocity control. A DS1104 data acquisition and control board from dSPACE was used to implement the PID control law for the DC motor and to collect the data.

In computations of the roots of polynomial equation (28) for different conditions and in a working range of velocities, it was found that there was only one real root and that it was positive. The other roots were two pairs of complex conjugates.

Fig. 2 shows the frequency of generation $f = \omega_e^* / 2\pi$ as a function of capacitance for different speeds, as well as for different loading conditions, all obtained using the theoretical analysis and compared to experimental data.

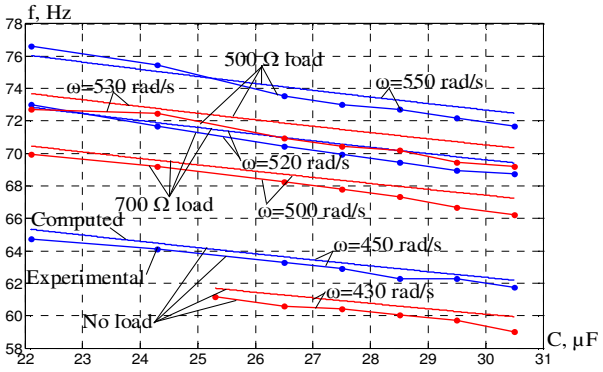

Fig. 2. Steady-state frequency as a function of capacitance for different velocities and loading conditions.

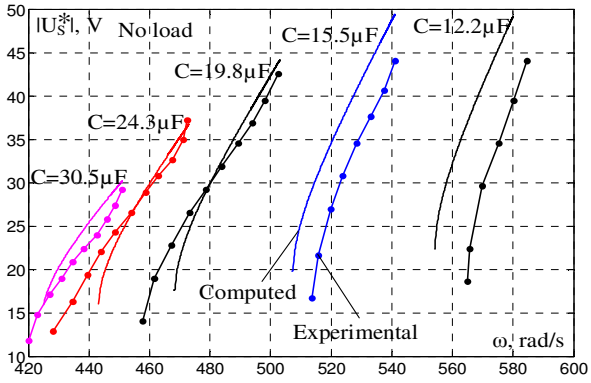

Fig. 3. Steady-state stator voltage amplitude as a function of velocity for different capacitor values.

The steady-state stator voltage amplitude is shown in Fig. 3 as a function of velocity for different capacitor values. When two values of i_M^* were possible, the one corresponding to the descending part of the magnetizing curve was used for the plots. Accuracy of the computation is not as good as in the previous plots, as it depends greatly on the accuracy of approximation of the magnetizing curve.

B. Stability of operating modes

The eigenvalues of the matrix A^* in (36) (with the specific choice of (40)) were computed in the velocity range from 424.5 rad/s to 925.1 rad/s, where L_M^* did not exceed L_{MAX}, and for the unloaded generator with 30.5 μF capacitor. The 6 eigenvalues always had the following characteristics: four were couples of complex conjugates with negative real parts, one had a non-zero real value and one had zero value. The zero eigenvalue is associated with the infinite number of equilibrium states and does not affect stability in a substantial way: there is no mechanism to lock the phase of the voltages and currents to an arbitrary time reference as in a grid-connected generator. A drift in phase also does not cause any problem. It was found that the complex

eigenvalues did not change greatly with velocity, and were well into the stable side of the plane. The main factor influencing the stability was therefore the real eigenvalue (referred to as #5), which was closer to the imaginary axis.

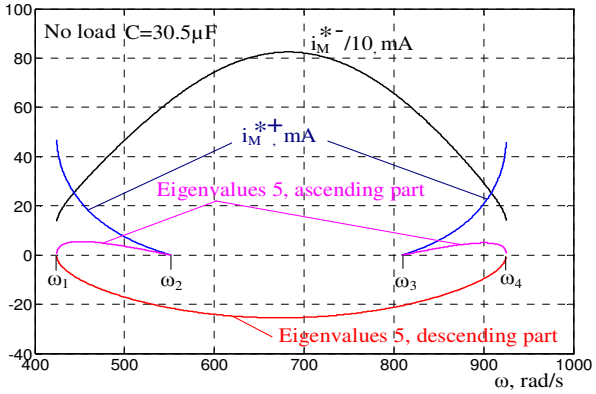

Fig. 4. Eigenvalue 5 as function of velocity for both the descending and the ascending parts of the magnetizing inductance curve.

Fig. 4 shows the possible solutions i_M^* and their associated eigenvalue 5 over a range of speeds. One finds that eigenvalue 5 is stable for all velocities in the case corresponding to the descending part. The plot of eigenvalue 5 for the ascending part is quite different from the descending part and only exists in a smaller range. It is always unstable. Overall, one finds that there are five speed regions with boundaries labeled ω_1, ω_2, ω_3, and ω_4. Referring to the discussion of section II.D, the velocity ranges correspond to the following cases:

- $\omega < \omega_1$ and $\omega > \omega_4$ correspond to case 1: there is no stable steady-state magnetizing current other than zero.
- $\omega_1 < \omega < \omega_2$ and $\omega_3 < \omega < \omega_4$ correspond to case 2: there is a stable large magnetizing current, but also a smaller unstable magnetizing current. Self-excitation must be triggered to reach a magnetizing current greater than or equal to the small i_M^*, for example by using pre-charged capacitors.
- $\omega_2 < \omega < \omega_3$ corresponds to case 3: there is a single stable magnetizing current. Spontaneous self-excitation will occur in this range due to small initial conditions such as residual flux.

Note that the speed range of Fig. 4 extends well beyond the rated speed of the motor. For larger motors, operating limits may restrict generation to the leftmost side of the range. Also, cases were found where the velocity range from ω_2 to ω_3 did not exist for some values of capacitance and load. In such cases, only triggered self-excitation is possible.

IV. Conclusions

The paper proposed a nonlinear dynamic model for an induction generator connected to resistive loads and capacitors. Using the model, it was found that the induction generator always had a zero equilibrium, in addition to either one stable nonzero equilibrium, or two equilibrium with one stable and one unstable. The operating velocity range was thus found to be divided into three types. The first one is such that self-excitation is not possible. The second type is such that self-excitation is possible, but needs to be triggered by reaching a magnetizing current greater than or equal to the one associated with the unstable equilibrium. Such triggering can be obtained using pre-charged capacitors or enforcing a sufficiently high level of residual flux. The third type is such that self-excitation is spontaneous, meaning that arbitrarily small initial conditions can trigger the self-excitation. The results unify and extend previous theories of self-excitation, in addition to providing new insights into its mechanisms.

References

[1] S.S. Murthy, O.P. Malik, & A.K. Tandon, "Analysis of self-excited induction generators," *IEE Proc.,* vol. 129, pt. C, no. 6, 1982, pp. 260-265.

[2] S.S. Murthy, B. Singh, & A.K.Tandon, "Dynamic models for the transient analysis of induction machines with asymmetrical connection," *Electr. Mach. and Electromech.*, 1981, no. 6, pp. 479-492.

[3] N.H. Malik & A.K. Al-Bahrani, "Influence of the terminal capacitor on the performance characteristics of a self excited induction generator," *IEE Proc.*, vol. 137, no. 2, 1990, pp. 168-173.

[4] A.K. Tandon, S.S.Murthy, & G.J.Berg, "Steady-state analysis of capacitor self-excited induction generators," *IEEE Trans. Power Apparatus and Systems*, vol. 103, no. 3, 1984, pp. 612-618.

[5] L. Ouazene & G. McPherson Jr., "Analysis of the isolated induction generator," *IEEE Trans. Power Apparatus and Systems*, vol. 102, no. 8, 1983, pp. 2793-2798.

[6] J.M. Elder, J.T. Boys & J.L. Woodward, "Self-excited induction machine as a small low-cost generator," *IEE Proc*., Pt. C, vol. 131, no. 2, 1984, pp. 33-41.

[7] S.M. Alghuwainem, "Steady-state analysis of an isolated self-excited induction generator driven by regulated and unregulated turbine," *IEEE Trans. Energy Conversion,* vol. 14, no. 3, 1999, pp. 718-723.

[8] C. Grantham, D. Sutanto, & B. Mismail, "Steady-state and transient analysis of self-excited induction generators," *IEE Proc.,* vol. 136, pt. B, no. 2, 1989, pp. 61-68.

[9] T.F. Chan, "Capacitance requirements of self-excited generators," *IEEE Trans. Energy Conversion*, vol. 8, no. 2, 1993, pp. 304-311.

[10] O. Ojo, "Minimum airgap flux linkage requirement for self-excitation in stand-alone induction generators," *IEEE Trans. Energy Conversion*, vol. 10, no. 3, 1995, pp. 484-492.

[11] S.-C. Kuo & L. Wang, "Dynamic eigenvalue analysis of a self-excited induction generator feeding an induction motor," *Winter Meeting of the IEEE Power Engineering Society*, vol. 3, 2001, pp. 1393 - 1397.

[12] M. Bodson & O. Kiselychnyk, "Analytic conditions for spontaneous self-excitation in induction generators," *Proc. of the American Control Conference*, Baltimore, MD, pp. 2527-2532, 2010.

[13] J.M. Elder, J.T. Boys, & J.L.Woodward, "The process of self excitation in induction generators," *IEE Proc.,* vol. 130, pt. B, no. 2, 1983, pp.103-108.

[14] D. Seyoum, C. Grantham, & F. Rahman, "The dynamic characteristics of an isolated self-excited induction generator driven by a wind turbine," *IEEE Trans. Industry Applications,* vol. 39, no. 4, 2003, pp. 936-944.

[15] M. Bodson & O. Kiselychnyk, "On the triggering of self-excitation in induction generators," *Proc. of the 20th International Symposium on Power Electronics, Electrical Drives, Automation and Motion (Speedam 2010)*, Pisa, Italy, pp. 866-871, 2010.

[16] E. Levi, "A unified approach to main flux saturation modeling in d-q axis models of induction machines," *IEEE Trans. Energy Conversion,* vol. 10, no. 3, 1995, pp. 455-461.

[17] E. Levi, "Main flux saturation modeling in double-cage and deep-bar induction machines," *IEEE Trans. Energy Conversion,* vol. 11, no. 2, 1996, pp. 305-311.